

Dark Matter Density Spikes around Primordial Black Holes

Yu. N. Eroshenko^{1,*}

¹*Institute for Nuclear Research, Russian Academy of Sciences,
pr. 60-letiya Oktyabrya 7a, Moscow, 117312 Russia*

(Dated: September 24, 2018)

We show that density spikes begin to form from dark matter particles around primordial black holes immediately after their formation at the radiation-dominated cosmological stage. This follows from the fact that in the thermal velocity distribution of particles there are particles with low velocities that remain in finite orbits around black holes and are not involved in the cosmological expansion. The accumulation of such particles near black holes gives rise to density spikes. These spikes are considerably denser than those that are formed later by the mechanism of secondary accretion. The density spikes must be bright gamma-ray sources. Comparison of the calculated signal from particle annihilation with the Fermi-LAT data constrains the present-day cosmological density parameter for primordial black holes with masses $M_{\text{BH}} \geq 10^{-8} M_{\odot}$ from above by values from $\Omega_{\text{BH}} \leq 1$ to $\Omega_{\text{BH}} \leq 10^{-8}$, depending on M_{BH} . These constraints are several orders of magnitude more stringent than other known constraints.

1. INTRODUCTION

Primordial black holes (PBHs), the possibility of whose formation was predicted in [1] and [2], can give valuable information about processes in the early Universe [3–5], in particular, about the shape of the perturbation spectrum on small scales [6]. The quantum evaporation of low-mass PBHs is important from the viewpoint of investigating fundamental processes at high energies [7] and can have significance for the theory of primordial nucleosynthesis and gamma-ray astronomy. In addition, PBHs can offer new possibilities for the formation of quasars at high z [8] and for baryonic objects with chemical peculiarities [9, 10]. Being captured by neutron stars, PBHs can affect their evolution, which gives a constraint on the number of PBHs [11]. In this paper, we will discuss only the PBHs that are formed during the collapses of adiabatic density perturbations, when a mixture of relativistic particles collapses into a PBH at the instant the perturbation crosses the cosmological horizon [12]. Note, however, that other PBH formation models have also been proposed at early dust-like stages [13, 14] or through the collapses of domain walls [15], [16, 17].

PBHs can themselves represent dark matter (DM) [18] if they are formed in sufficiently large quantities, but they can also serve as seeds for the formation of DM clumps [19–24]. Secondary accretion (generally, this mechanism was developed in cold DM onto a PBH [25], when DM flows toward the PBH and is virialized at some radius to form a halo, is usually considered in investigating DM clumps around PBHs. In this paper, we will show that the DM density around PBHs can reach much greater values than that under secondary accretion. This stems from the fact that in the thermal velocity distribution there are DM particles with low velocities that remain in finite orbits around PBHs and are not involved in

the overall cosmological expansion. The accumulation of such particles around PBHs gives rise to density spikes (halos).

Two regimes of density spike formation around PBHs are possible at the radiation-dominated stage. In the first case, which occurs for PBHs with masses $M_{\text{BH}} \leq 40 M_{\odot}$, PBHs are formed before the kinetic decoupling of DM particles (under the assumption that the DM particles are neutralinos with masses $m \sim 70$ GeV). In the interval between the PBH formation and kinetic decoupling, a DM overdensity has time to be formed around the PBH. As will be shown below, the exact form of this initial density distribution does not play a big role, while the separation of DM particles immediately after their kinetic decoupling is important. After their kinetic decoupling, the DM particles begin to fly apart in the PBH gravitational field, having some velocity distribution (a deformed Maxwell distribution). Some of the particles with low velocities remain gravitationally bound to the PBH, forming subsequently a density spike around it. In the second case, if $M_{\text{BH}} > 40 M_{\odot}$, such a PBH is formed already after the kinetic decoupling of DM particles, and there is no initial overdensity of radiation and DM around the PBH. In this case, the DM particles with low velocities also remain in finite orbits around the PBH, producing a density spike. Thus, DM density spikes are formed around PBHs at the radiation-dominated stage. After the onset of the matter-dominated stage in the Universe, the DM mass around PBHs begins to grow during the secondary accretion, and a universal density profile $\rho \propto r^{-9/4}$ is formed.

The DM density in the central regions of the spikes is so large that by now the DM particles have managed to annihilate (under the assumption that standard neutralinos constitute the DM) at distances that exceed the gravitational PBH radii by several orders of magnitude. For this reason, to calculate the present-day density profile around PBHs, it will be sufficient for us to consider the phenomena at great distances from the PBHs, where Newtonian gravitational dynamics is a good approxima-

* e-mail: eroshenko@inr.ac.ru

tion and the general relativity effects are unimportant. The DM remaining at great distances continues to annihilate at present, producing signals in gamma-ray emission. Comparison of the calculated signals with the Fermi-LAT data allows the number of PBHs to be constrained.

The annihilation of DM particles in clumps around PBHs has already been considered in [23, 24, 26], where constraints on the cosmological PBH density parameter were obtained. Calculations [23] and [24] assumed the density profile in the central region of a clump to be close to $\rho \propto r^{-3/2}$, while [26] considered power-law profiles $\rho \propto r^{-\alpha}$ with $\alpha = 1.5 - 3$. The annihilation of DM in density cusps around black holes was considered in [27], [28], [29], and new gamma-ray constraints were obtained. The goal of this paper is to calculate the density profile in the central region of DM clumps around PBHs by taking into account the initial thermal velocity distribution of DM particles after their kinetic decoupling. We will show that the density profile has a more complex form than $\rho \propto r^{-\alpha}$. Knowledge of the density profile allows one to calculate the signals from DM annihilation around PBHs more reliably and to obtain constraints on the number of PBHs in the Universe.

2. EVOLUTION OF THE DENSITY AROUND PBHs BEFORE KINETIC DECOUPLING

Consider the PBH formation at the radiation-dominated cosmological stage [12], when the equation of state for the matter in the Universe is $p = \rho c^2/3$. A thermalized mixture of photons and ultrarelativistic particles called radiation for short collapses into a PBH. If nonrelativistic DM particles are already present at this time in the Universe, then they move in the overall gravitational potential and, in addition, can interact with radiation. As an example, consider DM particles in the form of neutralinos with masses $m \simeq 70$ GeV. At early times, when the temperature was high, $T \geq 0.05mc^2$, neutralinos were in chemical equilibrium with radiation, i.e., the production of neutralinos and their pair annihilation were equiprobable. As the Universe cooled down, neutralinos dropped out of chemical equilibrium with radiation but still continued to efficiently interact with it through scatterings. The neutralino gas temperature was maintained at the radiation temperature level, and neutralinos could be entrained by radiation flows, for example, by the flow toward an accreting PBH. Finally, on further cooling of the radiation to some temperature T_d , whose value depends on the character of elementary interactions, the kinetic decoupling of DM particles from the radiation occurs at the time t_d , and the DM particles subsequently move freely only under the influence of gravitational forces. We will find the fraction of the DM particles that remain gravitationally bound to the PBH (have finite orbits) as they fly apart in the next section, while first it is necessary to discuss the initial DM density profile around the PBH before kinetic decoupling.

The mechanism for the formation of a DM density spike depends on the relation between the formation time of the PBH determined by its mass and the time t_d dependent on the character of interaction between DM particles and radiation. The PBH in some perturbed region is formed at the instant t_H this region crosses the cosmological horizon, which depends on the total mass M_H of the matter inside this region:

$$t_H \simeq \frac{GM_H}{c^3} = 2.6 \times 10^{-13} \left(\frac{M_{\text{BH}}}{10^{-8} M_\odot} \right) \text{ s}. \quad (1)$$

We take into account the fact that the mass M_{BH} of the forming PBH in the model of [12] is $M_{\text{BH}} = M_H/3^{3/2}$. The age of the Universe is related to the radiation temperature as

$$t = \frac{2.4}{\sqrt{g_*}} \left(\frac{T}{1 \text{ MeV}} \right)^{-2} \text{ s}, \quad (2)$$

where g_* is the number of degrees of freedom; therefore, the dependence of M_{BH} on T at t_H is

$$M_{\text{BH}} \simeq 40 \left(\frac{g_*}{10} \right)^{-1/2} \left(\frac{T}{27 \text{ MeV}} \right)^{-2} M_\odot. \quad (3)$$

The normalization factor in (3) is chosen to correspond to the temperature of the kinetic decoupling of neutralinos with masses $m \simeq 70$ GeV [30]

$$T_d \simeq 27 \left(\frac{m}{70 \text{ GeV}} \right)^{1/4} \left(\frac{\tilde{M}}{0.2 \text{ TeV}} \right) \left(\frac{g_*}{10} \right)^{1/8} \text{ MeV}, \quad (4)$$

which occurs at a time

$$t_d \simeq 10^{-3} \left(\frac{m}{70 \text{ GeV}} \right)^{-1/2} \left(\frac{\tilde{M}}{0.2 \text{ TeV}} \right)^{-2} \left(\frac{g_*}{10} \right)^{-3/4} \text{ s}, \quad (5)$$

where \tilde{M} is the supersymmetry parameter [30]. Thus, the mass of $\sim 40M_\odot$ given by Eq. (3) is a boundary value. If $M_{\text{BH}} < 40M_\odot$, then the kinetic decoupling of neutralinos occurs already after the PBH formation, while the radiation flow accreted onto the PBH entrained DM particles from the PBH formation time to t_d . If $M_{\text{BH}} > 40M_\odot$, then the neutralinos at the PBH formation time were free and moved independently from the radiation. The radiation could outflow from some region of space, while the DM remained in this region.

Consider the case of $M_{\text{BH}} < 40M_\odot$. We can single out the near zone bounded by the radius of influence of the PBH $r_{\text{infl}}(t)$ in which the PBH mass is equal to the radiation mass $M_{\text{BH}} = (4\pi/3)\rho_\infty(t)r_{\text{infl}}^3$, where $\rho_\infty(t) = 3/(32\pi Gt^2)$. Hence

$$r_{\text{infl}}(t) = (8GM_{\text{BH}}t^2)^{1/3}. \quad (6)$$

In dimensionless units,

$$\begin{aligned} \xi &= \frac{r_{\text{infl}}}{r_g} = \frac{c^2 t^{2/3}}{G^{2/3} M_{\text{BH}}^{2/3}} = \\ &= 7.4 \times 10^6 \left(\frac{M_{\text{BH}}}{10^{-8} M_\odot} \right)^{-2/3} \left(\frac{t}{10^{-3} \text{ s}} \right)^{2/3}, \quad (7) \end{aligned}$$

where $r_g = 2GM_{\text{BH}}/c^2$ is the gravitational PBH radius. We see that the PBH influence becomes relatively strong at low masses M_{BH} and long times t . The DM mass within the radius of influence is

$$M_{\text{DM}}(t) \simeq M_{\text{BH}} \left(\frac{t}{t_{\text{eq}}} \right)^{1/2} = 2 \times 10^{-8} M_{\text{BH}} \left(\frac{t}{10^{-3} \text{ s}} \right)^{1/2}, \quad (8)$$

where $t_{\text{eq}} \approx 2.4 \times 10^{12} \text{ s}$ is the transition time of the Universe from the radiation-dominated cosmological stage to the dust-like stage. In the region of influence the particles move in the PBH gravitational field, while outside the region of influence the cosmological expansion continues, though, of course, this separation is approximate and, in reality, there is a transition region. Note that the radius of the cosmological horizon at the radiation-dominated stage $r_H = 2ct$ is close to the radius of influence r_{infl} only near the PBH formation time, while later $r_H = 2ct$ expands faster than r_{infl} . Therefore, all of the processes we consider occur on scales much smaller than the size of the cosmological horizon.

The density distribution around a PBH could be accurately calculated through numerical hydrodynamic simulations similar to the simulations of PBH formation [31–34]. However, if the phenomena are considered not in the immediate vicinity of the PBH formation time but some time after, when the wave processes will damp out, then the approximation of quasi-stationary accretion can be used [35, 36]. Before the recombination epoch, photons are often scattered by baryons and are thermalized. This leads to two effects. First, a bulk flow velocity toward the PBH appears in such a continuous medium, though individual photons are not captured by the PBH. Second, although the expansion in the near zone is not the Friedmann one, partial density equalization near the PBH and at great distances occurs due to the existence of a high pressure. The radiation density near the PBH is largely determined by the density at great distances, while the local density growth near the PBH driven by its gravity is smoothed out strongly. Equalization must occur at distances from the PBH smaller than the sound horizon $r \ll r_s = 2ct/\sqrt{3}$, which is close in order of magnitude to the cosmological horizon. At these distances, the approximation of quasi-stationary accretion [35, 36] can be used for estimates.

According to [36], the distribution of an accreting fluid with the equation of state $p = \rho c^2/3$ is

$$\rho = \rho_{\infty}(t) \left[z + \frac{1}{3(1-1/\xi)} \right]^2, \quad (9)$$

where $\xi = r/r_g$,

$$z = \begin{cases} 2\sqrt{\frac{a}{3}} \cos\left(\frac{2\pi}{3} - \frac{\omega}{3}\right), & 1 \leq \xi \leq 3/2, \\ 2\sqrt{\frac{a}{3}} \cos\left(\frac{\omega}{3}\right), & \xi > 3/2, \end{cases} \quad (10)$$

$$\omega = \arccos \left[\frac{b}{2(a/3)^{3/2}} \right], \quad (11)$$

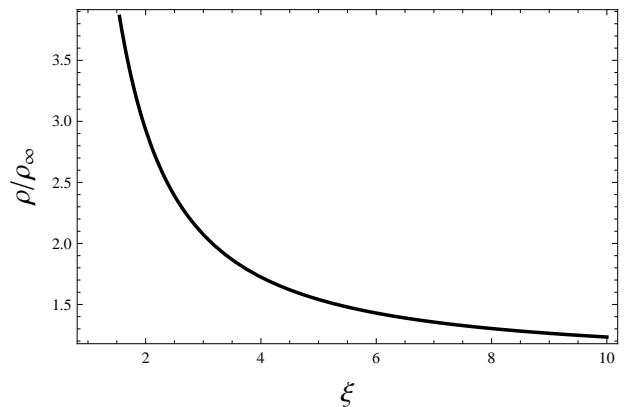


Figure 1. Density of a gas with the equation of state $p = \rho c^2/3$ near a black hole versus radial variable $\xi = r/r_g$ in the approximation of quasi-stationary accretion.

$$a = \frac{1}{3\left(1 - \frac{1}{\xi}\right)^2}, \quad b = \frac{2}{27\left(1 - \frac{1}{\xi}\right)^3} - \frac{27}{4\left(1 - \frac{1}{\xi}\right)\xi^4}. \quad (12)$$

The function (9) is shown in Fig. 1.

The formalism developed by [36] allows the velocity in the flow $u \equiv dr/ds$ to be found:

$$4u\xi^2 \left(\frac{\rho}{\rho_{\infty}} \right)^{3/4} = -A, \quad (13)$$

where $A = 2 \times 3^{3/2}$. At great distances $\xi \gg 3$, the solution (9) has asymptotics $\rho \simeq \rho_{\infty}(t)/(1 - 1/\xi)^2$, i.e., the density differs little from the mean cosmological density. In this case, according to (13), the hydrodynamic flow velocity $v \sim c/\xi^2$. This quantity is much smaller than the DM particle velocities that we will consider below. Thus, in the Newtonian region $r \geq 10r_g$ before the kinetic decoupling of DM particles, the density growth and the velocity anisotropy may be neglected. In contrast, in the case of $M_{\text{BH}} > 40M_{\odot}$, the PBH is formed already after kinetic decoupling, and the DM density distribution is not related to the radiation density growth around the PBH even in the near zone.

Consider the diffusive outflow of photons from a region of enhanced density, the Silk effect (see, e.g., [37]), which leads to an additional smoothing of the radiation and DM mass excess around the PBH before kinetic decoupling. The photon mean free path is $l_{re} = 1/(n_e\sigma_T)$, where σ_T is the Thomson cross section, and the electron number density in the cosmic plasma is

$$n_e \simeq \frac{\rho_{\text{eq}}\Omega_b t_{\text{eq}}^{3/2}}{m_p t^{3/2}}, \quad (14)$$

$\Omega_b \approx 0.045$. The Silk length $\lambda_S \simeq (l_{re}r_H)^{1/2}$ in dimensionless units is

$$\frac{\lambda_S}{r_g} = 1.5 \times 10^5 \left(\frac{t}{10^{-3} \text{ s}} \right)^{3/4} \left(\frac{M_{\text{BH}}}{10^{-8} M_{\odot}} \right)^{-1}, \quad (15)$$

i.e., the Silk effect can smooth out and reduce the radiation density in the central region of a future DM halo. This smoothing region has a size that is smaller than the total halo size by several orders of magnitude.

3. STREAMING OF DARK MATTER PARTICLES AFTER KINETIC DECOUPLING

Let us now consider the DM density growth around a PBH after the time of kinetic decoupling t_d , when the DM particles become free. The velocity distribution of DM particles far from the PBH is

$$f(\vec{v})d^3v = \frac{m^{3/2}}{(2\pi kT)^{3/2}} e^{-\frac{mv^2}{2kT}} d^3v, \quad (16)$$

where

$$T(t) = T_d \frac{t_d}{t} \quad \text{at} \quad t > t_d \quad (17)$$

in view of the decrease in the momentum of free particles $p \propto 1/a(t)$. Near the PBH at distances $r \leq 10r_g$, the distribution of particles differs noticeably from (16) due to the increase in radiation density compared to the homogeneous cosmological background and because of the existence of a bulk flow velocity toward the PBH. However, we restrict our analysis to the regions with $r \geq 10r_g$ in which, as was shown in Section 2, these corrections are insignificant. Therefore, we will use (16) in our subsequent calculations.

Let the PBH under consideration be at the coordinate origin. Denote the initial distance of some DM particle from the center by r_i and its initial velocity by \vec{v}_i . The particle energy is then $E = mv_i^2/2 + U(r_i)$, where $U(r) = -GmM_{\text{BH}}/r$. If the particle has an angular momentum $l = mr_i v_i \sin \theta_i$ (see Fig. 2), then the eccentricity of its orbit is [38]

$$e = \sqrt{1 + \frac{2El^2}{G^2 M_{\text{BH}}^2 m^3}}. \quad (18)$$

Let us consider some point B in Fig. 2 at distance r from the center and find the conditions that some particle from the initial distribution (16) will be in a finite orbit around the PBH after kinetic decoupling and will contribute to the DM density at point B. The first condition $E < 0$ means that the initial velocity is less than the escape velocity,

$$v_i < \left(\frac{2GM_{\text{BH}}}{r_i} \right)^{1/2}. \quad (19)$$

The second condition implies that the distance r lies between the minimum and maximum particle distances from the center,

$$r_{\text{min}} = a(1 - e) \leq r \leq r_{\text{max}} = a(1 + e), \quad (20)$$

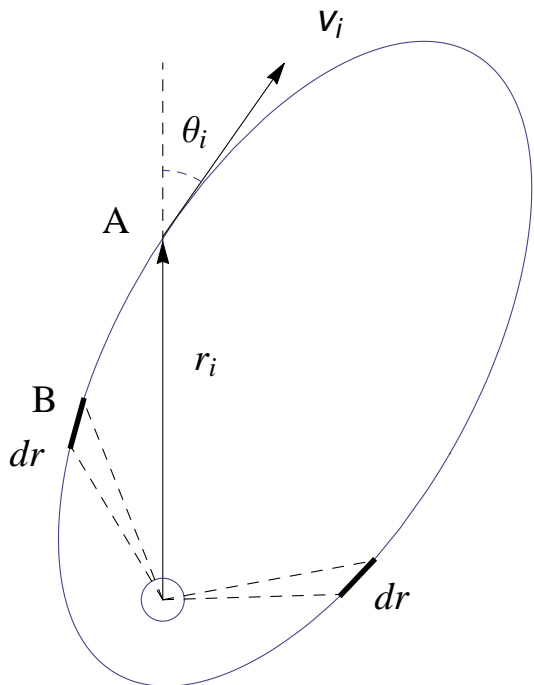


Figure 2. An example of a particle orbit around a PBH passing through point B. The contribution of all such orbits to the DM density at point B at distance r from the center is calculated. The vector \mathbf{r}_i indicates the initial position of the particle at the instant it was within the radius of influence of the hole, while \mathbf{v}_i indicates the particle velocity at this instant.

where the semimajor axis of the orbit is (Landau and Lifshitz 1988)

$$a = \frac{GmM_{\text{BH}}}{2|E|}. \quad (21)$$

The double condition (20) after transformations takes the form

$$\sqrt{1 + \frac{2El^2}{G^2 M_{\text{BH}}^2 m^3}} \geq \left| 1 + \frac{2Er}{GM_{\text{BH}}m} \right|. \quad (22)$$

Let us introduce the notation

$$x = \frac{r}{r_i}, \quad \gamma = \frac{GM_{\text{BH}}}{r_i v_i^2}, \quad (23)$$

(22) will then be written as

$$\cos^2 \theta_i \geq \cos^2 \theta_m = 2x(x - 1)\gamma + 1 - x^2. \quad (24)$$

The particle in its orbital motion traverses the segment of radial distances from r to $r + dr$ (see Fig. 2) twice in the orbital period

$$T_{\text{orb}} = \frac{\pi GM_{\text{BH}} m^{3/2}}{2^{1/2} |E|^{3/2}}, \quad (25)$$

Therefore, the particle spends the fraction $2dt/T_{\text{orb}}$ of its time at distances from r to $r + dr$, where dt is the time it takes for the particle to be displaced from r to $r + dr$. Given the initial DM density $\rho_i(r_i)$, the final density $\rho(r)$ can be written as the relation

$$\rho(r)4\pi r^2 dr = \int 4\pi r_i^2 dr_i \rho_i(r_i) \int d^3v f(v) \frac{2(dt/dr)}{T_{\text{orb}}} dr, \quad (26)$$

where the derivative dt/dr is found from the equation of motion for a particle in an orbit (Landau and Lifshitz 1988),

$$\frac{dt}{dr} = \frac{1}{\sqrt{2m[E - U(r)] - l^2/r^2}}, \quad (27)$$

while, according to the results of Section 2, we assume the initial density $\rho_i(r_i)$ at distances $r \geq 10r_g$ to be approximately uniform and equal to the cosmological DM-density:

$$\rho_i(r_i) \simeq \rho_d \frac{t_d^{3/2}}{t^{3/2}}, \quad (28)$$

where

$$\rho_d \simeq \Omega_m \rho_{\text{eq}} \left(\frac{t_{\text{eq}}}{t_d} \right)^{3/2} \simeq 4.7 \times 10^3 \text{ g cm}^{-3} \quad (29)$$

and $\Omega_m \simeq 0.27$. The collisionless system under consideration is described by the Liouville equation, and the method being applied in this paper is equivalent to an approximate solution of this equation. Indeed, Eq. (26) expresses the density conservation law in phase space integrated over the momenta by taking into account the volume transformation in momentum space, which follows from the Liouville equation.

When integrating in (26) over r_i , we should separately consider the regions with $r_i \leq r_{\text{infl}}(t_d)$ and $r_i > r_{\text{infl}}(t_d)$, where the radius of influence is given by Eq. (6). The first region at the time t_d is entirely in the region of PBH influence, and the particles in this region have a common velocity distribution (16) with $T = T_d$ and a common density $\rho_i(r_i) \simeq \rho_d$. In contrast, at $r_i > r_{\text{infl}}(t_d)$, the region of influence gradually expands. For each radius r_i , the temperature T and density ρ_i are found from Eqs. (17) and (28), respectively, in which t is specified by the equation $r_{\text{infl}}(t) = r_i$. It should be noted that the kinetic decoupling of DM particles occurs not instantaneously, and the scatterings of particles during the transition period can slightly change the final density of the captured DM particles.

Inequalities (19) and (24) separate out the region in parameter space over which the integration in (26) is performed. It is convenient to divide this integral into two parts with $x < 1$ and $x \geq 1$. The internal integration over the velocity directions, i.e., over the angles $\cos \theta_i$, is done analytically, while the remaining double integrals over the initial radii r_i and the absolute values

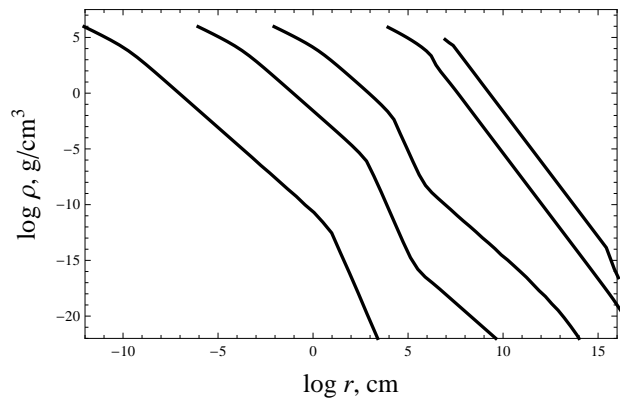


Figure 3. DM density around a PBH versus radius r for the following PBH masses (from left to right): $M_{\text{BH}} = 10^{-18}$, 10^{-12} , 10^{-8} , 10^{-2} , and $10M_{\odot}$.

of the initial velocities v_i are found by numerical methods. The maximum possible radii r_i are assumed to be equal to the radius of influence given by (7) at the time $t = t_{\text{eq}}$. At $t = t_{\text{eq}}$, a DM mass equal to the PBH mass is inside the region of PBH influence, and a DM halo is subsequently formed around the PBH by the mechanism of secondary accretion, when the PBH no longer determines the entire gravitational field but serves only as a small perturbation.

The results of our numerical calculations for various PBH masses are shown in Fig. 3. The numerical algorithm constructed in this paper gives an acceptable accuracy only in the range of masses $M_{\text{BH}} \sim (10^{-18} - 1)M_{\odot}$. The resulting density at small distances from the PBH exceeds ρ_d . This means that particles with low angular momenta are in eccentric orbits approaching the PBH at small radii. A universal behavior of the density at small radii, where there are segments with a density profile close to the power-law one r^{-1} , is also seen in Fig. 3 at $M_{\text{BH}} \leq 10^{-2}M_{\odot}$, but at large r the profile experiences a break due to the change of the regime of DM halo formation. The radii in Fig. 3 are shown formally starting from $r = 3r_g$. Strictly speaking, our calculations performed within the framework of Newtonian dynamics are applicable only at $r \geq 10r_g$. Therefore, the density at smaller radii must be considered as an estimate. In the next section, we will show that the density in the central region of the halo plays no role, because the DM in the central spikes has strongly annihilated by now and the density has decreased by several orders of magnitude.

4. EARLY PARTICLE ANNIHILATION IN SPIKES

If the DM particles are able to annihilate, then their density will decrease with time. As was shown in [39] and [40], the maximum DM density in a particular object at

the present time does not exceed

$$\rho_{\max} \simeq \frac{m}{\langle \sigma_{\text{ann}} v \rangle t_0} \simeq 9.4 \times 10^{-15} \left(\frac{m}{70 \text{ GeV}} \right) \times \quad (30)$$

$$\times \left(\frac{\langle \sigma_{\text{ann}} v \rangle}{3 \times 10^{-26} \text{ cm}^3 \text{ s}^{-1}} \right)^{-1} \left(\frac{t_0}{1.4 \times 10^{10} \text{ years}} \right)^{-1} \text{ g cm}^{-3},$$

where t_0 is the time elapsed since the formation of the object. The thermal production cross section for DM particles in the early Universe $\langle \sigma_{\text{ann}} v \rangle \simeq 3 \times 10^{-26} \text{ cm}^3 \text{ s}^{-1}$ is taken as a normalization for the annihilation cross section (see, e.g., [41]).

It follows from Fig. 3 that the density of the DM halo for all of the PBH masses considered at small radii exceeds considerably (30). This means that the dense central regions of the halo existed only at early epochs, while by now the DM density in the halos around PBHs has decreased to (30). An accurate calculation of the law of decrease in central density due to particle annihilation is a more complicated problem that is beyond the scope of this paper. Particles with different orbital parameters annihilate at each point of the density spike. Therefore, a self-consistent allowance for the decrease in DM density simultaneously in all regions of the density spike is needed for the calculation. Such a calculation is planned to be performed in future works. At early times, the annihilation-generated gamma-ray emission experienced absorption and thermalization in the cosmic plasma. The annihilation that continued during primordial nucleosynthesis or at the reionization epoch of the Universe could influence these processes, but the quantitative role of this influence requires a separate study. DM annihilation around PBHs is an additional factor that can lead to chemical anomalies in the baryonic halos around PBHs considered by [10].

Thus, DM density spikes, from which halos with a central density $\rho \sim \rho_{\max} \sim 10^{-14} \text{ g cm}^{-3}$ and a decreasing density on the periphery have been left at present, existed around PBHs. The sizes of these halos are equal in order of magnitude to the radii of PBH influence given by Eq. (6) at $t = t_{\text{eq}}$.

5. ANNIHILATION OF DARK MATTER AROUND PBHS AT THE PRESENT EPOCH, OBSERVATIONAL CONSTRAINTS

Consider the annihilation of DM particles in density spikes around PBHs that are located in our Galaxy at the present epoch. The annihilation in a spike around a single PBH, i.e., the number of annihilated particles per unit time

$$\dot{N} = 4\pi \int r^2 dr \rho^2(r) \frac{\langle \sigma_{\text{ann}} v \rangle}{m^2}, \quad (31)$$

where the profiles obtained in Section 3 by taking into account the early annihilation in the central part considered in Section 4 are used as the density profile in the

spike $\rho(r)$. Thus, starting from a radius of $\sim 3r_g$, we assume that $\rho(r) \sim \rho_{\max} = 10^{-14} \text{ g cm}^{-3}$, while at large radii, when the densities in Fig. 3 decrease to ρ_{\max} , the profiles shown in Fig. 3 are used under the integral in (31).

After the beginning of the dust-like stage of the Universe at $t > t_{\text{eq}}$, a DM halo begins to grow around the PBH at distances $r > r_{\text{infl}}(t_{\text{eq}})$ through the mechanism of secondary accretion [25]. Its density distribution is

$$\rho(r) \simeq 3 \times 10^{-21} \left(\frac{r}{1 \text{ pc}} \right)^{-9/4} \left(\frac{M_{\text{BH}}}{10^2 M_{\odot}} \right)^{3/4} \text{ g cm}^{-3}, \quad (32)$$

with the outer boundary of (32) being determined by the influence of ordinary inflationary density perturbations, so that the total mass of the DM halo around the PBH exceeds the PBH mass M_{BH} approximately by two orders of magnitude [19]. The density (32) does not exceed the halo density at $r = r_{\text{infl}}(t_{\text{eq}})$. Therefore, the outer halo (32) makes a minor contribution to (31), while the central region of the halo with density (30) and the parts of the halo adjacent to it shown in Fig. 3 make a major contribution.

The total annihilation signal from some direction characterized by the angle ψ with respect to the Galactic center is

$$J_{\gamma} = 2\eta_{\pi^0} \dot{N} \frac{\Omega_{\text{BH}}}{\Omega_m M_{\text{BH}}} \int dL \rho_{\text{H}}(r(L)), \quad (33)$$

where Ω_{BH} is the cosmological density parameter for PBHs with masses M_{BH} , $\eta_{\pi^0} \sim 10$ is the number of photons per π^0 decay, and the integration is along the line of sight. The hadronic annihilation channel, when most of the gamma-ray photons are emitted during the decays of neutral pions $\pi^0 \rightarrow 2\gamma$ produced by the annihilation of DM particles, is assumed to be the main one. As the density profile of the Galactic halo $\rho_{\text{H}}(r)$, we use the Navarro–Frenk–White profile [42]

$$\rho_{\text{H}}(r) = \frac{\rho_0}{(r/R_s)(1+r/R_s)^2}. \quad (34)$$

where $R_s = 20 \text{ kpc}$ and $\rho_0 = 6.7 \times 10^6 M_{\odot} \text{ kpc}^{-3}$.

Let us compare (33) calculated toward the Galactic anticenter $\psi = \pi$ (this gives the minimum signal and, accordingly, the most conservative constraint) with the Fermi-LAT observational constraint from the diffuse gamma-ray background $J^{\text{obs}}(E > m_{\pi^0}/2) = 1.8 \times 10^{-5} \text{ cm}^{-2} \text{ s}^{-1} \text{ sr}^{-1}$ [43]. The condition $J_{\gamma} < J^{\text{obs}}$ gives an upper bound on Ω_{BH} , which is shown in Fig. 4 together with several other known constraints on PBHs from [4]. In particular, these are the constraints from the Hawking radiation and microlensing and the constraint from the overall cosmological PBH density. These constraints are often expressed via the fraction β of the mass of the early Universe gone into PBHs at the time of their formation (1). The quantity β is related to Ω_{BH} as [4]

$$\Omega_{\text{BH}} \simeq 5 \times 10^{17} \beta \left(\frac{M_{\text{BH}}}{10^{15} \text{ g}} \right)^{-1/2}. \quad (35)$$

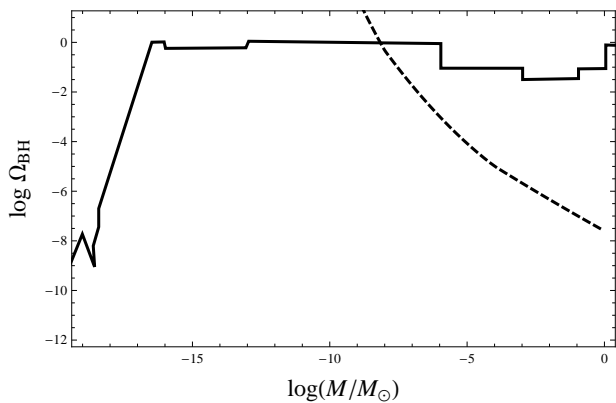


Figure 4. The solid curve indicates the known upper bounds on the cosmological PBH density parameter Ω_{BH} from Carr et al. (2010). The dashed curve indicates the constraints based on the DM particle annihilation effect obtained here.

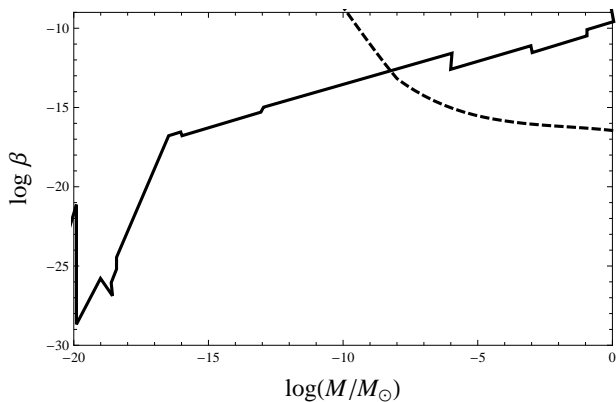


Figure 5. Same as Fig. 4 but for the fraction β of the mass of the Universe gone into PBHs at the time of their formation.

The constraint on β following from neutralino annihilation in density spikes is shown in Fig. 5.

We see from Figs. 4 and 5 that the constraint from annihilation at $M_{\text{BH}} \geq 10^{-8} M_{\odot}$ gives constraints on the number of PBHs that are several orders of magnitude more stringent than other known constraints.

6. CONCLUSIONS

DM clumps can be produced by various mechanisms [30]. They can be formed both from cosmological density perturbations in the dark matter itself and around compact seed masses, for example, around cosmic strings [44] or PBHs [19–24]. Secondary accretion, the infall and

virialization of cold DM onto PBHs, was thought to be the main mechanism for the formation of DM clumps around PBHs. However, we showed in this paper that there exists another mechanism that gives rise to denser DM clumps around PBHs than was considered in secondary accretion models.

The DM density around PBHs grows at the radiation-dominated stage due to the presence of slow DM particles in their thermal velocity distribution. Fairly slow particles after their kinetic decoupling are in finite orbits around PBHs and produce high-density DM clumps. Considering the kinematics of particles around PBHs allowed the density profile to be found. The DM particles in the central regions of clumps have managed to annihilate by now. However, the remaining halos are still very dense, and intense annihilation occurs in them. This effect can be interesting for experiments on indirect detection of DM particles though the search for their annihilation products, because the annihilation of particles in spikes can contribute to the observed gamma-ray emission. Comparison of the calculated signal with the Fermi-LAT observational limits gives upper bounds on the present-day cosmological PBH density parameter from $\Omega_{\text{BH}} \leq 1$ to $\Omega_{\text{BH}} \leq 10^{-8}$, depending on the PBH masses at $M_{\text{BH}} \geq 10^{-8} M_{\odot}$. Comparable (in magnitude) but weaker constraints $\Omega_{\text{BH}} \leq 10^{-4}$ were obtained previously in [23], where the density profile in a spike was assumed to be $\rho \propto r^{-3/2}$.

However, it should be noted that our constraints are largely model-dependent ones: they depend fundamentally on the as yet unknown properties of DM particles. The derived constraints refer to standard neutralinos or to other DM particles having the properties of weakly interacting massive particles (WIMPs), i.e., having masses and annihilation cross sections comparable to them in order of magnitude. For other DM particles, both the velocity distribution (16) and the annihilation signals can be significantly different. For example, if the DM particles do not annihilate at all, then the formation of a DM density spike around PBHs is still possible, but, in this case, there is no early annihilation and no decrease in central density and the signals are absent in the cosmic gamma-ray emission. The density spikes can be bright gamma-ray sources only at certain masses and annihilation cross sections of DM particles. The derived constraints do not refer, for example, to the models in which the DM consists of PBHs. Nevertheless, the neutralinos in nonminimal supersymmetric models so far remain among the most probable DM candidates, and the constraints obtained here can hold.

Author is grateful to V.K. Dubrovich for useful discussions.

[1] Ya. B. Zel'dovich and I. D. Novikov, *Sov. Astron.* 10, 602 (1967).

[2] S. Hawking, *Mon. Not. R. Astron. Soc.* 15, 75 (1971).

- [3] B. J. Carr, *Lect. Notes Phys.* 631, 301 (2003).
- [4] B. J. Carr, K. Kohri, Y. Sendouda, and J. Yokoyama, *Phys. Rev. D* 81, 104019 (2010).
- [5] K. M. Belotsky et al., *Mod. Phys. Lett. A* 29, 1440005 (2014).
- [6] A. S. Josan, A. M. Green, and K. A. Malik, *Phys. Rev. D* 79, 103520 (2009).
- [7] E. Bugaev and P. Klimai, *Phys. Rev. D* 79, 103511 (2009).
- [8] V. Dokuchaev, Yu. Eroshenko, and S. Rubin, *Grav. Cosmol.* 11, 99 (2005).
- [9] V. K. Dubrovich, *Astron. Lett.* 29, 6 (2003).
- [10] V. K. Dubrovich and S. I. Glazyrin, arXiv:1208.3999 [astro-ph.CO] (2012).
- [11] F. Capela, M. Pshirkov, and P. Tinyakov, *Phys. Rev. D* 87, 123524 (2013).
- [12] B. J. Carr, *Astrophys. J.* 201, 1 (1975).
- [13] M. Yu. Khlopov and A. G. Polnarev, *Phys. Lett. B* 97, 383 (1980).
- [14] N. A. Zabotin, P. D. Nasel'skii, and A. G. Polnarev, *Sov. Astron.* 31, 353 (1987).
- [15] V. A. Berezin, V. A. Kuzmin, and I. I. Tkachev, *Phys. Lett. B* 120, 91 (1983).
- [16] M. Yu. Khlopov, R. V. Konoplich, S. G. Rubin, and A. S. Sakharov, Preprint 1203 (I Roma University, 1998); arXiv:hep-ph/9807343.
- [17] S. G. Rubin, M. Yu. Khlopov, and A. S. Sakharov, *Grav. Cosmol.* 6, 51 (2000).
- [18] P. Ivanov, P. Naselsky, and I. Novikov, *Phys. Rev. D* 50, 7173 (1994).
- [19] V. I. Dokuchaev and Yu. N. Eroshenko, *Astron. Lett.* 27, 759 (2001).
- [20] M. Ricotti, *Astrophys. J.* 662, 53 (2007).
- [21] K. J. Mack, J. P. Ostriker, and M. Ricotti, *Astrophys. J.* 665, 1277 (2007).
- [22] M. Ricotti and A. Gould, *Astrophys. J.* 707, 979 (2009).
- [23] B. C. Lacki and J. F. Beacom, *Astrophys. J. Lett.* 720, L67 (2010).
- [24] R. Saito and S. Shirai, *Phys. Lett. B* 697, 95 (2011).
- [25] E. Bertschinger, *Astrophys. J. Supp. Ser.* 58, 39 (1985).
- [26] Z. Dong, *Mon. Not. R. Astron. Soc.* 418, 1850 (2011).
- [27] P. Sandick, J. Diemand, K. Freese, D. Spolyar, Proceedings of "Identification of Dark Matter 2010 (IDM 2010)"; arXiv:1012.0068 [astro-ph.CO].
- [28] P. Sandick, J. Diemand, K. Freese, D. Spolyar, *JCAP* 1101, 018 (2011); arXiv:1008.3552 [astro-ph.CO].
- [29] P. Sandick, J. Diemand, K. Freese, D. Spolyar, *Phys. Rev. D* 85, 083519 (2012); arXiv:1108.3820 [astro-ph.CO].
- [30] V. S. Berezhinsky, V. I. Dokuchaev, and Yu. N. Eroshenko, *Phys. Usp.* 57, 1 (2014).
- [31] B. J. Carr and S. W. Hawking, *Mon. Not. R. Astron. Soc.* 168, 399 (1974).
- [32] D. K. Nadyozhin, I. D. Novikov, and A. G. Polnarev, *Sov. Astron.* 22, 129 (1978).
- [33] I. D. Novikov, A. G. Polnarev, A. A. Starobinskii, and Ia. B. Zeldovich, *Astron. Astrophys.* 80, 104 (1979).
- [34] G. V. Bicknell and R. N. Henriksen, *Astrophys. J.* 232, 670 (1979).
- [35] F. C. Michel, *Astrophys. Space Sci.* 15, 153 (1972).
- [36] E. Babichev, V. Dokuchaev, and Yu. Eroshenko, *Phys. Rev. Lett.* 93, 021102 (2004).
- [37] L. E. Gurevich and A. D. Chernin, *Introduction to Cosmogony* (Nauka, Moscow, 1978).
- [38] L. D. Landau and E. M. Lifshitz, *Course of Theoretical Physics, Vol. 1: Mechanics* (Pergamon Press, New York, 1988).
- [39] V. S. Berezhinsky, A. V. Gurevich, and K. P. Zybin, *Phys. Lett. B* 294, 221 (1992).
- [40] J. Silk and A. Stebbins, *Astrophys. J.* 411, 439 (1993).
- [41] D. S. Gorbunov and V. A. Rubakov, *Introduction to the Theory of the Early Universe: Hot Big Bang Theory* (URSS, Moscow, 2008).
- [42] J. F. Navarro, C. S. Frenk, and S. D. M. White, *Astrophys. J.* 462, 563 (1996).
- [43] A. A. Abdo et al., *Phys. Rev. Lett.* 104, 101101 (2010).
- [44] E. W. Kolb and I. I. Tkachev, *Phys. Rev. D* 50, 769 (1994).